Measurement of vibrational line profiles in H_2–rare-gas mixtures: Determination of the speed dependence of the line shift

J. Ph. Berger, R. Saint-Loup, and H. Berger
Laboratoire de Physique, Université de Bourgogne, 21000 Dijon, France

J. Bonamy and D. Robert
Laboratoire de Physique Moléculaire, Université de Franche-Comté, 25030 Besançon Cedex, France
(Received 7 September 1993)

High-resolution inverse Raman experiments for H_2 diluted in Ar have revealed unusual Q-line profile features at various concentrations which have been interpreted in terms of speed-changing collisions. A more general approach including both speed- and phase-changing collisions has led to an alternative interpretation of these features. In order to further analyze the role of these various collisional mechanisms, new experiments have been performed. Pure H_2 and H_2 perturbed by Ne, Ar, and Xe have been investigated at various temperatures between 295 and 800 K.

PACS number(s): 33.70.Jg, 33.20.Fb

I. INTRODUCTION

Numerous studies have been devoted to vibrational line profiles of the hydrogen molecule in pure medium and in mixtures. These studies were largely motivated by the simplicity of its rovibrational spectrum and performed to get information on the collisional mechanisms in connection with the intermolecular potentials. At subatmospheric pressure, the well-known Dicke effect [1–3] due to velocity-changing collisions was exhaustively analyzed [4–6].

Recently, new features were observed by Farrow *et al.* [7] for H_2-Ar at pressures well above the Dicke minimum and interpreted in terms of speed-changing collisions. The main feature was the observation of a remarkable deviation from the usual linear mixing rule for the linewidth [i.e., $\gamma = c_A\gamma_A + (1-c_A)\gamma_{A\text{-}B}$, where γ_A and $\gamma_{A\text{-}B}$ are the collisional broadening parameters for the two kinds of colliders in proportions c_A and $1-c_A$, respectively]. An asymmetry of the H_2 vibrational line profile was also observed [7]. These spectral features were first interpreted [7] by accounting for both the inhomogeneity due to the radiator speed dependence of the line shift $\delta(v)$ and the narrowing exchange between the various speed groups through speed-changing collisions. A more general approach, including not only the roles of the speed changing and the dephasing collisions but also that of collisions changing both speed and phase, was proposed [8]. This generalization for the collisional mechanisms allows an alternative interpretation of the profile, based on the last two types of collisions only. Before presenting our experimental results, we will briefly recall the main characteristics of this general model and its two limit cases mentioned just above.

II. THE COLLISIONAL MODELS FOR THE Q-LINE PROFILE

In the model of Ref. [8], three types of collisions were considered: the dephasing collisions (D), the speed-changing ones (SC), and those changing both speed and phase (SCD). Let us summarize the role of these types of collisions on the spectral profile: dephasing collisions lead to an inhomogeneous profile through the speed-dependent line-shift coefficient $\delta_D(v)$ and the line broadening $\gamma_D(v)$; speed-changing collisions narrow and symmetrize this inhomogeneous line shape and are characterized by the speed-changing collision frequency ν_{sc} (assumed to be independent of the radiator speed v); the SCD collisions characterized by the speed-changing frequency parameter ν_{SCD} also induce narrowing and symmetrization of the inhomogeneous profile, which becomes Lorentzian with average parameters $\langle\delta_{SCD}(v)\rangle$ and $\langle\gamma_{SCD}(v)\rangle$ when the two previous types of collisions are inefficient. All the collisional parameters $\delta_D(v)$, $\gamma_D(v)$, ν_{SC}, ν_{SCD}, $\delta_{SCD}(v)$, and $\gamma_{SCD}(v)$ obviously follow the usual mixing rule with respect to the concentration.

From the kinetic equations and within the hard-collision approximation, the resulting analytical expression for the line profile is [8]

$$I(\omega)=\pi^{-1}\mathrm{Re}\left\{\frac{\langle[i\omega+F(v)]^{-1}\rangle}{1-\nu_{SC}\langle[i\omega+F(v)]^{-1}\rangle-\langle[\nu_{SCD}-\gamma_{SCD}(v)-i\delta_{SCD}(v)][i\omega+F(v)]^{-1}\rangle}\right\}, \quad (1)$$

where $F(v)=\nu_{SC}+\nu_{SCD}+\gamma_D(v)+i\delta_D(v)$ and ω is the detuning frequency. In Eq. (1), $\langle\ \rangle$ means an average over the radiator speed. Two limiting cases are of particular interest.

The first limit case corresponds to that proposed by Farrow *et al.* [7] and will be referred as FRSR in the following.

Only D and SC collisions are thus considered leading to the following line profile:

$$I(\omega)=\pi^{-1}\mathrm{Re}\left\{\frac{\langle\{\nu_{SC}+\gamma_D(v)+i[\omega+\delta_D(v)]\}^{-1}\rangle}{1-\nu_{SC}\langle\{\nu_{SC}+\gamma_D(v)+i[\omega+\delta_D(v)]\}^{-1}\rangle}\right\}. \tag{2}$$

Notice that the speed dependence of the line-broadening coefficient $\gamma_D(v)$ is also considered here.

This model is characterized by three physical parameters [ν_{SC}, $\delta_D(v)$, and $\gamma_D(v)$], which cannot be directly deduced from experiment. Their determination requires the measurement of the temperature dependence $\delta_D(T)$ and $\gamma_D(T)$ as well as a model for the relative speed dependence of these two coefficients [i.e., $\delta_D(v_{rel})$ and $\gamma_D(v_{rel})$; cf. Sec. V]. For this model, $\gamma_D(T)$ and $\delta_D(T)$ represent the collisional broadening and shifting coefficient, respectively [$\gamma_D(T)\equiv\gamma_{coll}(T)$ and $\delta_D(T)\equiv\delta_{coll}(T)$].

In the second limit case, only D and SCD collisions are thus considered and the line profile takes the form

$$I(\omega)=\pi^{-1}\mathrm{Re}\left\{\frac{\langle\{\nu_{SCD}+\gamma_D(v)+i[\omega+\delta_D(v)]\}^{-1}\rangle}{1-\langle[\nu_{SCD}-\gamma_{SCD}(v)-i\delta_{SCD}(v)]\{\nu_{SCD}+\gamma_D(v)+i[\omega+\delta_D(v)]\}^{-1}\rangle}\right\}. \tag{3}$$

We will term this model RTBT, since it has been established in Ref. [8] starting from the general expression (1). Let us define the fraction x of SCD collisions in terms of the total collision frequency

$$x=\nu_{SCD}/\nu_{tot} \quad \text{where } \nu_{tot}=\nu_{SCD}+\nu_D \tag{4}$$

and introduce the following definitions for the collisional line broadening $\gamma_{coll}(v)$ and line shifting $\delta_{coll}(v)$:

$$\gamma_{SCD}(v)=x\gamma_{coll}(v)\ ,\quad \delta_{SCD}(v)=x\delta_{coll}(v)\ ,$$
$$\gamma_D(v)=(1-x)\gamma_{coll}(v)\ ,\quad \delta_D(v)=(1-x)\delta_{coll}(v)\ . \tag{5}$$

The collisional broadening and shifting coefficients are given through thermal average

$$\gamma_{coll}(T)=\gamma_D(T)+\gamma_{SCD}(T)\ ,$$
$$\delta_{coll}(T)=\delta_D(T)+\delta_{SCD}(T)\ . \tag{6}$$

This model is characterized by four physical parameters x, ν_{tot}, $\gamma_{coll}(v)$, and $\delta_{coll}(v)$, but ν_{tot} can be reasonably identified as the velocity-changing collision frequency β. This parameter has been defined by Rautian and Sobel'man [9] as

$$\beta=kT/m\mathcal{D}\ , \tag{7}$$

where m is the mass of the radiator and $\mathcal{D}$ the diffusion coefficient of the two colliders. When D collisions are predominant (i.e., $x\ll 1$), the profile is strongly inhomogeneous and thus asymmetric. This is similar, but not identical, to the FRSR profile when ν_{SC} is small. In the opposite situation, only SCD collisions are efficient ($x=1$), the line profile is thus Lorentzian, and the Doppler effect is negligible in the density range considered.

This last feature constitutes the main difference between FRSR and RTBT models since in the former model the asymptotic Lorentzian behavior would be reached only in the extreme narrowing of the inhomogeneous profile by the speed-changing collisions (cf. Ref. [10]).

III. EXPERIMENTAL RESULTS

A. Experimental device

Inverse Raman spectroscopy was used to obtain the $Q(1)$ transition (near 4155 cm^{-1}) and the spectra were recorded with the Raman spectrometer of the Dijon University (Fig. 1). The probe beam is obtained from the 476-nm line of a single-mode argon laser which is actively stabilized by a Fabry-Pérot interferometer. The frequency jitter (initially about 20 MHz) was then reduced to 1 MHz. Because the Fabry-Pérot interferometer was temperature stabilized, the slow drift of the laser was reduced to about 30 MHz per hour. The pump source used a continuous tunable narrow bandwidth ring dye laser (1 MHz) which was pulse amplified (up to 200 kW) in a dye amplifier system (Spectra Physics PDA-1) pumped with a frequency-doubled single-mode Nd:YAG laser (where YAG denotes yttrium aluminum garnet).

The pump- and probe-laser beams were focused in the gas sample with a 30-cm focal-length lens. It can be noted that in order to avoid Stark effect, the highest peak intensity produced at the focus of the beams was kept below 2 GW/cm^2. However, at high concentrations of H_2, the gain is sufficient and it is not necessary to focus the laser beams. After the focalization in the gas cell, beams were then separated by an optical filter. The inverse Raman signal was detected by a fast photodiode, amplified, and stored in the data acquisition system.

A Michelson wavemeter provides accurate absolute

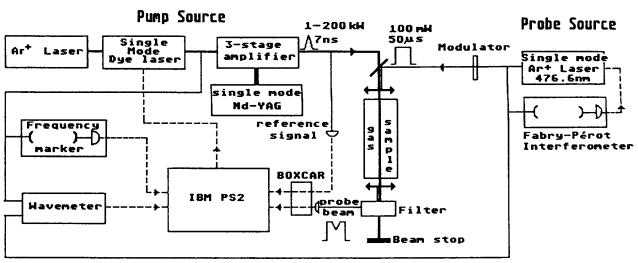

FIG. 1. Stimulated Raman device at the Dijon University.

measurements of both argon and dye lasers, owing to a reference He-Ne laser stabilized on hyperfine components of I_2. For each spectral scan of the dye laser, only the initial and final wavelengths of both lasers were measured with an accuracy of about 3 MHz. During the scan, the dye frequency was controlled by a confocal étalon, which is used as a frequency marker to correct the nonlinearity of the dye laser.

The gas sample was contained in a 10-mm-i.d. stainless-steel cylinder which was placed inside a heater. The gas cell was equipped with sapphire windows. The 6-mm-thick windows were cut with their C axes perpendicular to their faces. The cutting error amounted to about three angular degrees, and it was necessary to rotate the windows during assembly in order to correct the residual birefringence. The measurements were made at densities of nearly 10 amagat and at temperatures from 295 to 795 K and the investigated H_2 concentrations were roughly equal to 2%, 20%, 50%, and 80%. The transducer used for pressure measurements was continuously in contact with the gas sample but placed externally to the heater. Thus the pressure was controlled and measured for each spectrum with an accuracy of $\pm 0.3\%$. Gas densities were calculated in amagat units using the virial expression (limited to the second order). For H_2 mixtures, the second virial coefficient is given by

$$B_T = c_{H_2}^2 B_{H_2-H_2} + 2c_{H_2}c_{Per}B_{H_2-Per} + c_{Per}^2 B_{Per-Per} \cdot \quad (8)$$

Most of the second virial coefficients for the mixtures were derived from experiments [11,12]. The others were calculated according to Ref. [13]. The magnitude of the largest virial correction to the density was found for the highly dilute H_2-Xe mixture and was equal to 6% above ideal gas density (at 296 K and 10 atm). For the other mixtures, corrections were less than 1%. Temperatures were measured with thermocouples accurate to ± 2.5 K from 295–600 K and to $\pm 0.75\%$ of the temperature (expressed in °C) above 600 K. The temperature was monitored with two thermocouples which were not in physical contact with the gas volume. Indeed, the first one was near the heater and the other one was located in a small hole made in the cell and centered on the sample gas volume. With another configuration of the vessel, we measured the real temperature by locating a thermocouple exactly at the gas volume center in order to avoid systematic temperature measurement errors. The measurement discrepancies between this thermocouple and the one placed outside the gas volume (in the small hole) were found to be equal to 4 K at 450 and 600 K and equal to 5 K at 800 K. Note that we observed nearly the same temperature discrepancies whatever the mixture (although the thermal conductivities of the various mixtures are strongly different). The temperature corrections due to these discrepancies were taken into account in the following. As a consequence of the errors on pressure and temperature, the density error was estimated to be less than 1.5%.

B. Line-shift measurements

The frequency at the peak of the line exhibits a nonlinear behavior vs perturber concentration which increases with temperature. This deviation from the usual linear mixing rule $[\delta = c_A\delta_A + (1-c_A)\delta_{A-B}]$ is due to the asymmetric profile (Fig. 2). This asymmetry requires us to consider the center of gravity of the line to deduce the experimental shift. This effectively suppresses the previously mentioned nonlinearity for the shift and will

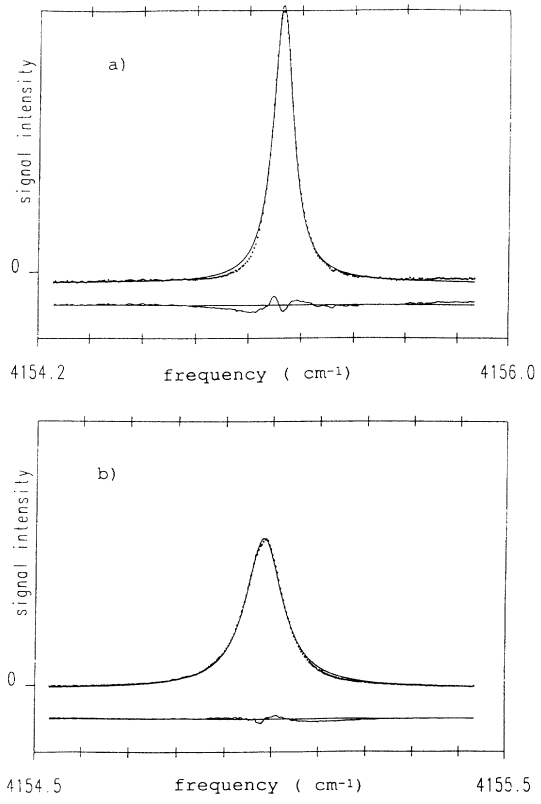

FIG. 2. Experimental IRS spectra (data points) of the $Q(1)$ line at 295 K when the perturber is (a) neon or (b) xenon. The spectra are fitted with a Lorentzian profile (dashed lines).

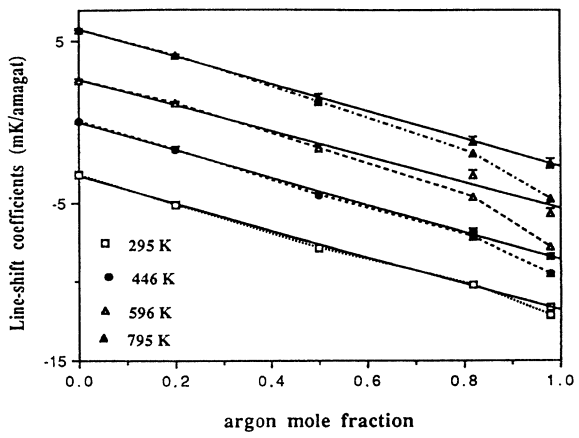

FIG. 3. The line-shift coefficients (symbols) are reported versus the argon mole fraction for several temperatures. Nonlinearities are observed if one considers the line peak (dotted line). They disappear for the center of gravity of the line (solid line).

TABLE I. Collisional line-shift coefficients (in 10^{-3} cm^{-1}/amagat), for H_2-H_2, H_2-Ne, H_2-Ar, and H_2-Xe mixtures (100% rare-gas mole fraction) at several temperatures. The numbers in parentheses indicate experimental uncertainties in the last digit(s).

	295 K	400 K	446 K	500 K	596 K	795 K
H_2-H_2	−3.32(10)		−0.03(15)		2.57(15)	5.80(15)
H_2-Ne	5.14(20)		8.17(20)		10.95(20)	13.18(20)
H_2-Ar	−11.82(20)		−8.35(20)		−5.39(25)	−2.73(25)
H_2-Xe	−37.6(3)	−35.6(4)		−33.7(5)		

be discussed below. It thus allows us to get accurate values for δ_A and δ_{A-B}. Consequently, the usual mixing rule has been used to determine the H_2–rare-gas collisional shift coefficients at several temperatures (Table I). An example of the discrepancies observed between the line shift obtained from the line peak frequency position and the line shift obtained from the center of gravity position is shown in Fig. 3. These discrepancies are only significant for highly dilute H_2-Ar mixtures. Notice that in the experimental conditions of Ref. [7] (i.e., a 50% concentration), the measurement of the shift from the line maximum was realistic.

C. Linewidth measurements

The experiments have been carried out for densities about $\rho=10$ amagat, well above the Dicke minimum equal to ~2.7, 1.1, 1.0, and 0.7 amagat when the perturbers are H_2, Ne, Ar, and Xe, respectively [4–6]. For H_2–heavy-rare-gas mixtures, the residual Doppler linewidth is negligible. Below a 50% perturber concentration, the observed profiles are symmetric and well fitted by a Lorentzian shape, allowing the direct determination of the broadening coefficient $\Gamma(T)$. For pure H_2 and for the H_2-He mixture, the residual Doppler effect must then be accounted for in this "Dicke regime" [1]. The broadening coefficient $\Gamma(T)$ is thus given in hertz by

$$\Gamma(T)=\gamma_{\rm obs}(T)-\frac{2\pi\mathcal{D}\nu_R^2}{c^2\rho}\ , \tag{9}$$

where $\gamma_{\rm obs}(T)$ is the half width at half maximum (HWHM) of the observed Lorentzian line shape, c the speed of light, and ν_R the Raman frequency. For highly diluted H_2 mixtures, the line profiles are asymmetric. For asymmetric spectra, broadening coefficients $\Gamma(T)$ are found to be significantly larger than those determined from a Lorentzian description of the line shape. Figure 4 shows the dependence on the perturber mole fraction of the observed line width at room temperature for several perturbers. The variation of the linewidth vs perturber concentration at different temperatures for H_2-Ar is given in Fig. 5. Above a 50% perturber concentration, a nonlinearity of the HWHM is evidenced. This nonlinear behavior increases vs temperature.

IV. COMPARISON WITH OTHER RESULTS

In Tables II and III our measured values for the line shift and the linewidth are compared to previous results [7,14–18]. Bischel and Dyer [14] have studied the temperature dependence of the pure H_2 Raman linewidth and line shift for the $Q(0)$ and $Q(1)$ transitions for temperatures between 77 and 450 K and in a density range from 1 to 50 amagat. The data reported at 295 K and

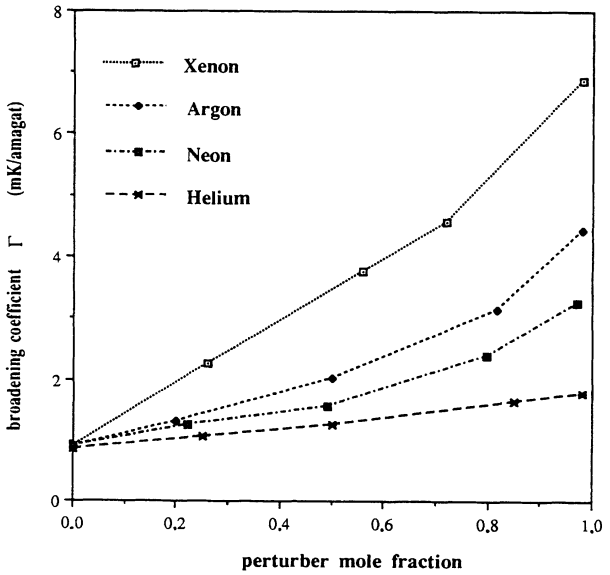

FIG. 4. Experimental HWHM $Q(1)$ broadening coefficient Γ versus the perturber mole fraction for several H_2-X mixtures at 295 K (X=He,Ne,Ar,Xe).

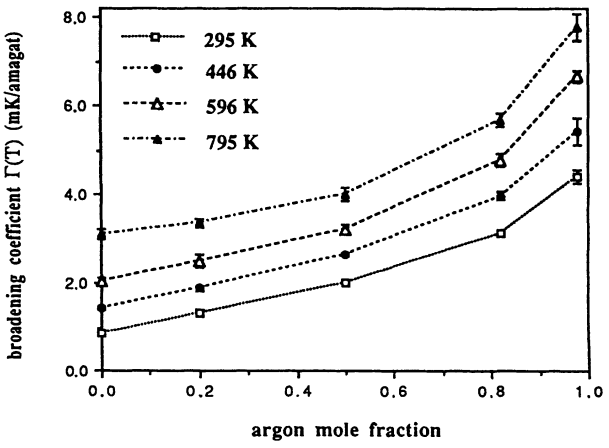

FIG. 5. Experimental HWHM $Q(1)$ broadening $\Gamma(T)$ coefficient for H_2-Ar versus the argon mole fraction, at several temperatures.

TABLE II. Comparisons between line-shift coefficients expressed in 10^{-3} cm^{-1}/amagat at 100% rare-gas mole fraction. The numbers in parentheses indicate uncertainties in the last digit(s). At 450, 750, and 1000 K, our values are interpolated or extrapolated from our measurements at 295, 446, 596, and 795 K.

	295 K				450 K				750 K		1000 K	
	This work	Previous works			This work	Previous works			This work	Previous works	This work	Previous works
H_2-H_2	−3.32(10)	−3.20(5)[a]	−3.20(4)[b]	−2.95(20)[c]	0.05(10)	0.70(5)[a]	0.05(6)[b]	0.57(20)[c]	5.13(20)	5.85(8)[e]	8.61(20)	9.16(11)[a]
H_2-Ne	5.14(20)	4.4(3)[d]										
H_2-Ar	−11.82(20)	−12.0(1)[e]	−13.5(4)[c]		−8.35(20)	−8.2(1)[e]	−11.8(4)[c]		−3.24(20)	−2.7(2)[e]	0.30(30)	0.86(40)[e]
H_2-Xe	−37.6(3)	~−30[d]										

[a]Reference [15].
[b]Reference [14].
[c]Reference [16].
[d]Reference [17].
[e]Reference [7].

450 K exhibit an excellent agreement with ours.

More recently, Rahn and Rosasco [15] realized a similar study. At room temperature good agreement with our data for the line shift is observed, but at high temperatures their values are significantly larger than ours. Because of those differences, we have studied the possibility of systematic errors in our temperature measurements. To do this, a thermocouple was introduced in the cell exactly at the center of the gas volume in order to avoid systematic temperature measurement errors. The measurement discrepancies between this thermocouple and the one placed outside the gas volume (in the small hole) were found to be equal to 4 K at 450 and 600 K and equal to 5 K at 800 K. The error concerning our results (Table II) includes the previously discussed systematic temperature error.

In order to minimize the error of measurement, the spectrum of pure H_2 has been recorded several times and at different times throughout our studies of H_2 mixtures. For the linewidths, the values measured from 295 to 1000 K are in agreement with ours (see Table III).

Let us note that a study of the pure H_2 Q branch ($J=0-5$) was recently realized from 295 to 1000 K. At high temperature, the comparison with the results of Refs. [15] and [18] leads to the same observations as for the $Q(1)$ transition, i.e., significant discrepancies for the line-shift coefficients and agreement for the linewidth coefficients. The other values for pure H_2 were obtained from less accurate techniques [7,14,16]. This explains the observed discrepancies.

For the mixture H_2-Ar, data of Ref. [7] are in reasonable agreement with ours, accounting for the fact that the relative uncertainties are larger at high temperature. For the data of Ref. [16], the same remark as that above holds.

V. SPEED DEPENDENCE OF COLLISIONAL LINE SHIFT AND LINE-BROADENING COEFFICIENTS

For most molecules, in the impact regime, the shift and broadening speed dependence is usually disregarded. For

TABLE III. Comparisons between measured HWHM expressed in 10^{-3} cm^{-1}/amagat for 100% rare-gas mole fraction. The numbers in parentheses indicate uncertainties in the last digit(s). At 450, 725, and 1000 K our values are interpolated or extrapolated from our measurements at 295, 446, 596, and 795 K. The data labeled by d have been deduced from calculations through Eq. (2) using the values for collision broadening and narrowing coefficients given in Ref. [7].

	295 K			450 K			725 K		1000 K	
	This work	Previous work		This work	Previous works		This work	Previous works	This work	Previous works
H_2-H_2	0.87(5)	0.87(5)[a]	0.87(2)[b]	1.44(5)	1.55(3)[a]	1.44(3)[b]	2.72(10)	2.84(5)[a]	4.31(15)	4.28(9)[a]
H_2-Ne	3.25(15)	2.7(3)[c]								
H_2-Ar	4.42(13)	~4.6[d]							8.95(20)	~10.0[d]
H_2-Xe	6.90(20)	~8[c]								

[a]Reference [18].
[b]Reference [14].
[c]Reference [17].
[d]Reference [7].

H_2–rare gas, the mentioned nonlinearity of the linewidth vs concentration (Fig. 4) and the asymmetric line profile for diluted mixtures require the accounting for this speed dependence (cf. Sec. II).

A. Collisional line shift

The following empirical expression for the relative speed dependence of the dephasing shift cross section has been used in Ref. [7] with the FRSR model

$$\sigma_{\text{coll}}(v_{\text{rel}})=av_{\text{rel}}+b+c/v_{\text{rel}} , \tag{10}$$

with a, b, and c being three adjustable parameters. The corresponding temperature dependence for the shift is straightforwardly obtained from Eq. (10) through a Boltzmann average of $v_{\text{rel}}\sigma_{\text{coll}}(v_{\text{rel}})$,

$$\delta_{\text{coll}}(T)=a\overline{v_{\text{rel}}^2}+b\bar{v}_{rel}+c\equiv AT+B\sqrt{T}+C , \tag{11}$$

where $\bar{v}_{\text{rel}}=\sqrt{8kT/\pi\mu}$, with μ being the reduced mass of the two colliders.

The radiator speed-dependent shift coefficient appearing in Eq. (2) is obtained from a *partial* Boltzmann average of $v_{\text{rel}}\sigma_{\text{coll}}(v_{\text{rel}})$ with the distribution $f(\vec{v}+\vec{v}_{\text{rel}},T)$ over $\vec{v}_{\text{rel}}$,

$$\delta_{\text{coll}}(v,T)=\int f(\vec{v}+\vec{v}_{\text{rel}},T)v_{\text{rel}}\sigma(v_{\text{rel}})d\vec{v}_{\text{rel}} . \tag{12}$$

Equations (10) and (12) lead to

$$\delta_{\text{coll}}(y,T)=a\overline{v_p^2}e^{-y^2}M(\tfrac{5}{2},\tfrac{3}{2},y^2) +b\bar{v}_p e^{-y^2}M(2,\tfrac{3}{2},y^2)+c , \tag{13}$$

where $\bar{v}_p$ means the average speed of the perturber ($\bar{v}_p=\sqrt{8kT/\pi m_p}$), $y=v/\bar{v}_p$ ($\bar{v}_p$ being the most probable perturber speed $\bar{v}_p=\sqrt{2kT/m_p}$), and $M(\,)$ is the confluent hypergeometric function [19]. A more convenient expression is given in terms of the error function [20] $\Phi(y)$

$$\delta_{\text{coll}}(y,T) =a\overline{v_p^2}\left[1+\frac{2y^2}{3}\right] +b\bar{v}_p\left[\frac{e^{-y^2}}{2}+\left[\frac{\sqrt{\pi}}{4y}+\frac{y\sqrt{\pi}}{2}\right]\Phi(y)\right]+c . \tag{14}$$

In Ref. [7], the line-shift coefficients were determined by measuring the $Q(1)$ line in a 50% H_2-Ar mixture allowing to fit the profile by a Lorentzian shape. The v average shift $\delta_{\text{coll}}(T)$ was thus assumed to be approximately equal to the maximum frequency for the considered line. We have seen that if such a procedure is used for higher argon concentration, a nonlinearity of the line shift then appears (cf. Fig. 3). The use of the center of gravity $\delta_G(T)$ for the observed line (i.e., its first moment) suppresses this nonlinearity and permits us to assume that, for all concentrations, $\delta_{\text{coll}}(T)\cong\delta_G(T)$. A justification for this approximation is given in the Appendix. Thus the a, b, and c parameters are determined by fitting $\delta_{\text{coll}}(T)$ [Eq. (11)] to $\delta_G(T)$ experimentally measured (Table I) using a least-squares procedure.

The empirical expression (10) has been found unrealistic. Indeed, at very high temperature, the first contribution becomes predominant. This requires a positive value for the a parameter due to the repulsive nature of the intermolecular forces at high collision energy. The fitting procedure has led to a negative a coefficient for all the considered mixtures as well as for pure H_2. An alternative empirical expression for the temperature dependence of $\delta_{\text{coll}}(T)$, found proportional to $\sqrt{T}$ (Fig. 6), is suggested in this paper. So, a consistent expression for the shift cross section is

$$\sigma_{\text{coll}}(v_{\text{rel}})=b+c/v_{\text{rel}} \tag{15}$$

leading to

$$\delta_{\text{coll}}(T)=\langle\delta_{\text{coll}}(y,T)\rangle=b\bar{v}_{\text{rel}}+c\equiv B\sqrt{T}+C . \tag{16}$$

Experimental values for B and C coefficients are given in Table IV. As physically expected, B is positive and C is negative for all the molecular pairs.

B. Collisional linewidth

The collisional linewidth unlike the line shifts cannot be deduced directly from experiments (cf. the Appendix), but requires the calculation of the line shape from a theoretical model (FRSR or RTBT). This calculation starting from Eqs. (2) and (3) needs the knowledge of the two B and C coefficients through the expression of the shift in terms of the reduced speed ($y=v/\bar{v}_p$)

$$\delta_{\text{coll}}(y,T) =B\sqrt{\mu/m_p}\sqrt{T}\left[\frac{e^{-y^2}}{2}+\left[\frac{\sqrt{\pi}}{4y}+\frac{y\sqrt{\pi}}{2}\right]\Phi(y)\right]+C . \tag{17}$$

We have analyzed our experimental data by neglecting, as in Ref. [7], the speed dependence of the linewidth [i.e.,

TABLE IV. Parameters B and C of expression (16) fitted through a least-squares procedure to the experimental line shifts (cf. Table I).

Parameter	H_2-H_2	H_2-Ne	H_2-Ar	H_2-Xe
B (10^{-3} cm^{-1} K$^{-1/2}$ amagat^{-1})	0.823	0.739	0.835	0.770
C (10^{-3} cm^{-1} amagat^{-1})	−17.41	−7.442	−26.11	−50.96

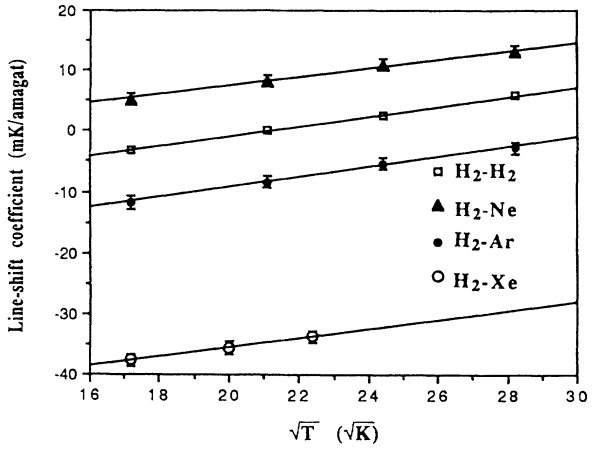

FIG. 6. The line-shift coefficients measured for several H_2-X mixtures ($X=H_2$,Ne,Ar,Xe) are reported (symbols) versus the temperature square root. These data have been modeled by straight lines.

$\gamma(v,T)\equiv\gamma(T)$]. The characteristic physical parameters for the two models [i.e., $(\gamma_{\text{coll}}^{\text{FRSR}},\nu_{\text{SC}})$ for the FRSR model and $(\gamma_{\text{coll}}^{\text{RTBT}},\nu_{\text{SCD}})$ for the RTBT one] are obtained from a least-squares fit between the calculated [from Eq. (2) or (3)] and experimental broadening coefficients [$\Gamma(T)$].

1. *Pure H_2*

In this case, the two parameters cannot be determined from symmetric experimental spectra for the two following reasons. A large range of values for ν_{SC} or x leads to symmetric calculated profiles (when ν_{SC} is one order larger than γ_{D} or when $0.9<x<1$) and the two parameters γ_{coll} and ν_{SC} or x are strongly correlated. So, we have set ν_{SC} and x by assuming that all collisions are efficient for changing the speed of radiator (in other words, each velocity-changing collision also changes the speed); thus we have set x equal to 1 and ν_{SC} equal to β [Eq. (7)]. Let us note that this assumption was made by Farrow *et al.* [7] only at 295 K; at 1000 K, they have set ν_{SC} equal to 60(±20)% of β. The results (Table V) obtained for the two models from this same assumption are basically different. Indeed, as said before in the RTBT model, when x is equal to 1, the profile is homogeneous and consequently the broadening coefficient Γ exactly corresponds to γ_{coll}. In the model FRSR when ν_{SC} is equal to β, an inhomogeneous broadening remains and γ_{coll} is close but not equal to the broadening coefficient Γ (cf. the Appendix).

2. *H_2–rare-gas mixtures*

For H_2–rare-gas mixtures, the pairs of parameters $[(\gamma_{\text{coll}}^{\text{FRSR}},\nu_{\text{SC}})$ and $(\gamma_{\text{coll}}^{\text{RTBT}},\nu_{\text{SCD}})]$ for the two models have been determined from Eqs. (2) or (3) and (17), using a linear mixing rule. Both FRSR and RTBT models lead to consistent description of the concentration dependence of the observed HWHM at each considered temperature (Fig. 7). The corresponding characteristic parameters $(\gamma_{\text{coll}}^{\text{FRSR}},\nu_{\text{SC}})$ or $(\gamma_{\text{coll}}^{\text{RTBT}},\nu_{\text{SCD}})$ are given in Table V. The choice of a different law for $\delta_{\text{coll}}(T)$ with respect to that of Ref. [7] [Eq. (15) instead of Eq. (10)] explains the observed significant differences with parameters of Ref. [7] for H_2-Ar.

The temperature dependence of $\gamma_{\text{coll}}(T)$, in the above assumption consisting in disregarding the v dependence, is given in Fig. 8. This temperature dependence is correctly reproduced by the linear law

$$\gamma_{\text{coll}}(T)=A'T+C' . \tag{18}$$

To deduce the speed dependence law of the collisional broadening, we have proceeded along the same way as for the collisional shift [cf. Eq. (15)]. Accounting for Eq. (18) we have introduced the following expression for the broadening cross section vs v_{rel}:

$$\sigma(v_{\text{rel}})=a'v_{\text{rel}}+c'/v_{\text{rel}} , \tag{19}$$

with the coefficients a' and c' being related to A' and C' by

TABLE V. Parameters for the H_2-X mixtures ($X=H_2$,Ne,Ar,Xe) for 100% rare-gas mole fraction adjusted from the RTBT and the FRSR models to obtain the best agreement with the experimental linewidths at different perturber concentrations.

	295 K				400 K	446 K			500 K	596 K			795 K		
	H_2-H_2	H_2-Ne	H_2-Ar	H_2-Xe	H_2-Xe	H_2-H_2	H_2-Ne	H_2-Ar	H_2-Xe	H_2-H_2	H_2-Ne	H_2-Ar	H_2-H_2	H_2-Ne	H_2-Ar
Parameters of the RTBT model															
γ_{coll} (mK/amagat)	0.87	1.7	2.35	5.0	5.0	1.48	2.4	2.8	5.0	2.04	3.3	3.2	3.1	4.2	3.4
x	1.0	0.15	0.12	0.08	0.1	1.0	0.15	0.12	0.1	1.0	0.16	0.11	1.0	0.16	0.11
$\nu_{\text{SCD}}=x\beta$ (mK/amagat)	47.0	9.3	10.9	10.4	13.7	52.0	11.1	11.0	14.5	55.0	13.0	12.3	58.0	14.2	13.9
Parameters of the FRSR model															
$\gamma_{\text{D}}=\gamma_{\text{coll}}$ (mK/amagat)	0.7	1.5	2.1	4.5	4.5	1.22	2.1	2.5	4.5	1.7	3.0	2.8	2.7	4.0	3.1
ν_{SC} (mK/amagat)	47.0	10.0	11.0	8.0	10.0	52.0	10.0	12.0	13.0	55.0	12.0	12.0	58.0	14.0	12.0

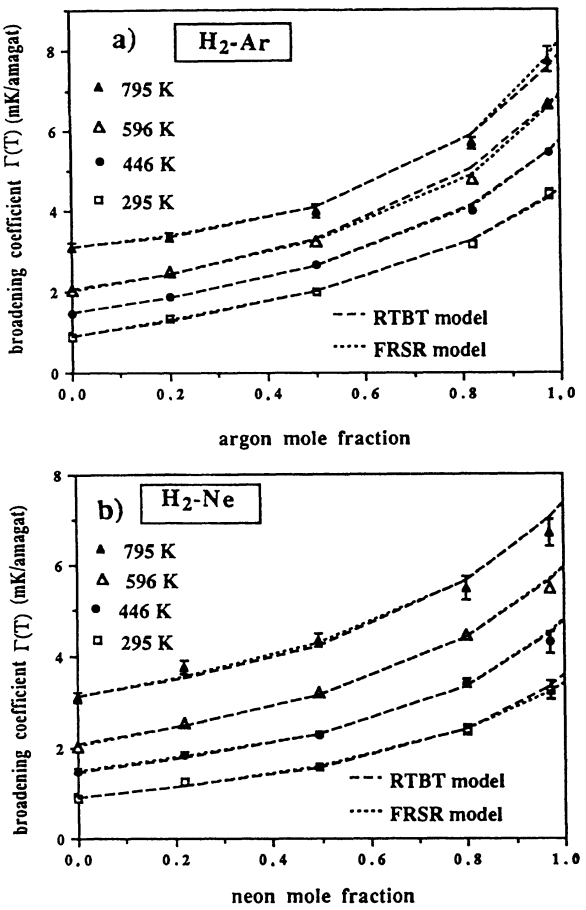

FIG. 7. The experimental (symbols) and calculated (dotted lines) HWHM $\Gamma(T)$ versus the perturber mole fraction at various temperatures. The perturbers are (a) argon and (b) neon.

$$A'=\frac{3k}{\mu}a' \ , \quad C'=c' \ .$$

The resulting speed dependence of the collisional broadening coefficient is

$$\gamma_{\text{coll}}(y,T)=a'\bar{v}_p^2 e^{-y^2}M(\tfrac{5}{2},\tfrac{3}{2},y^2)+c' \ . \tag{20}$$

Introducing Eqs. (20) and (17) into Eq. (2) or (3) following the model considered, it is in principle possible to deduce, from experiments, the speed dependence of the line broadening coefficient knowing that of the line shift [i.e., B and C coefficients in Eq. (17)]. This requires the determination of the three parameters A', C', and ν_{sc} for the FRSR model (or ν_{SCD} for RTBT) by a least-squares fit procedure of the calculated profile with the experimental one. Unfortunately, the signal-to-noise ratio and the correlation existing between these three parameters has not allowed a consistent determination of the speed dependence of γ_{coll}.

VI. DISCUSSION

Apart from the nonlinearity of the line broadening coefficient for H_2–rare-gas mixtures vs concentration evidenced previously [7], the present work has shown that the shift of the asymmetric line maximum exhibits the same feature. The origin of this shift nonlinearity has been clearly explained and the use of the first-order moment of the line, restoring the linearity, has been justified.

The experimental study shows that the temperature dependence of this line shift is $BT^{1/2}+C$. Thus the empirical form for the $Q(1)$ shift cross section averaged over impact parameter as a function of relative velocity is $\sigma(v_{\text{rel}})=b+cv_{\text{rel}}^{-1}$. The resulting dependence of this shift vs the radiator speed v has been deduced from the determination of the B and C coefficients.

The two models considered (FRSR and RTBT), accounting for such a v dependence of the shift and for the collisional narrowing exchange between the various speed groups, lead to a consistent description of the line-broadening nonlinearity for all the molecular pairs H_2-X. The line-broadening coefficient, assumed to be v independent, has been determined as a function of temperature. It exhibits a variation in $A'T+C'$. The coefficients γ_{coll}

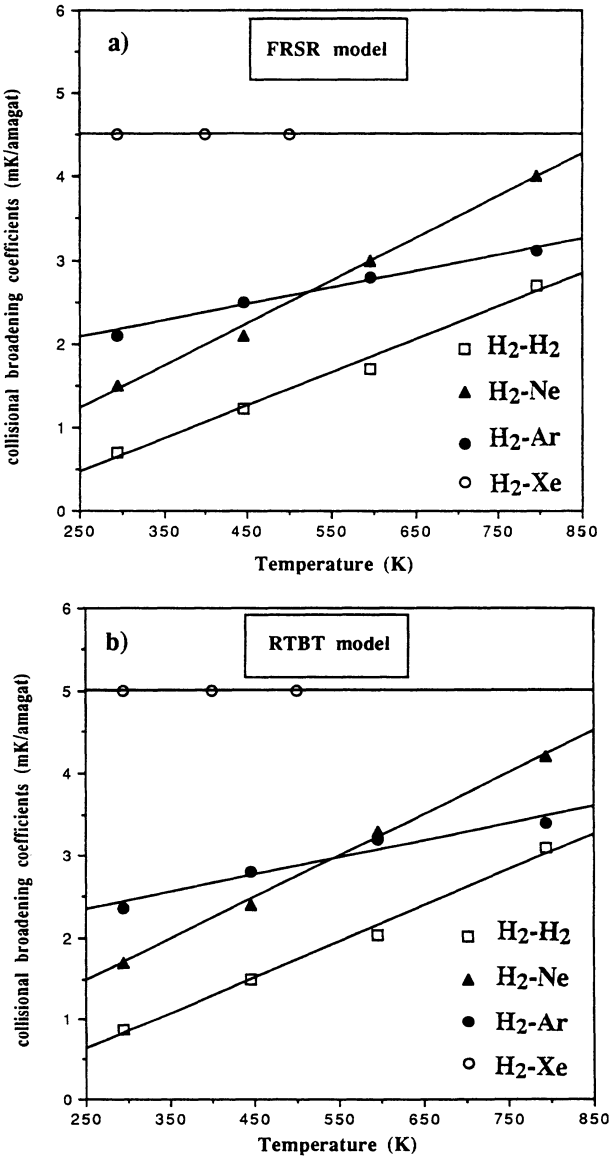

FIG. 8. Collisional line broadening coefficients ($\gamma_{\text{coll}}^{\text{FRSR}}$ or $\gamma_{\text{coll}}^{\text{RTBT}}$) versus temperature for the different mixtures. A linear temperature dependence is observed.

for the FRSR and RTBT models are close, with $\gamma_{\text{coll}}^{\text{RTBT}}$ being about 10% larger than $\gamma_{\text{coll}}^{\text{FRSR}}$ for all H_2–rare-gas mixtures. Notice that in the RTBT model, due to the assumed 100% rate of speed changing and dephasing collisions for pure H_2, γ_{coll} is exactly equal [8] to the experimental Γ value. A residual inhomogeneous broadening, as in the FRSR model [7], would be obtained for $x < 1$, leading to a concomitant change of the $\gamma_{\text{coll}}^{\text{RTBT}}$ parameter for H_2–rare gases.

These collisional broadening parameters may be compared to the available calculated values. Semiclassical calculations of Refs. [17] and [21] for H_2-Ar at room temperature are larger by a factor of 2. But an empirical parameter characterizing the vibrational dependence of the repulsive part of the potential was adjusted to obtain agreement with the experimental width Γ instead of γ_{coll}, obtained with the two speed-dependent models (RTBT or FRSR). More recently, accurate close-coupling calculations [22] using a refined intermolecular potential determined from van der Waals complexes spectra [23] have been achieved for H_2-Ar and D_2-Ar. In contrast with calculations for HCl-Ar [24], D_2-He [25–27], and CO-He [28] leading to a good agreement with experiments, significant discrepancies with respect to $\gamma_{\text{coll}}(T)$ were obtained for H_2-Ar [22]. Neither the amplitude nor the temperature dependence is reproduced. This is particularly true for the shift, for which the discrepancy reaches one order of magnitude at 1000 K. An explanation of such a disagreement could be the inaccuracy of the potential surface used, but further theoretical analyses are needed.

ACKNOWLEDGMENTS

The authors would like to thank CNES, CNRS, and SEP for financial support. The Laboratoire de Physique is URA CNRS No. 1796, and the Laboratoire de Physique Moléculaire is URA CNRS No. 772.

APPENDIX

The FRSR and RTBT profiles can be expressed in terms of $S(\omega)$ and $R(\omega)$ as

$$I_{\text{FRSR}}(\omega)=\text{Re}\left\{\frac{S(\omega)}{1-\nu_{\text{SC}}S(\omega)}\right\}\equiv\text{Re}\left\{\frac{1}{\mathcal{A}(\omega)}\right\}, \tag{A1}$$

and

$$I_{\text{RTBT}}(\omega)=\text{Re}\left\{\frac{S(\omega)}{1-R(\omega)}\right\}\equiv\text{Re}\left\{\frac{1}{\mathcal{B}(\omega)}\right\}, \tag{A2}$$

where

$$S(\omega)=\int_0^\infty \frac{f(v)dv}{i\omega+\nu+\gamma_D(v)+i\delta_D(v)}, \tag{A3}$$

$\nu\equiv\nu_{\text{SC}}$ for FRSR, $\nu\equiv\nu_{\text{SCD}}$ for RTBT, $f(v)$ is the Boltzmann function, and

$$R(\omega)=\int_0^\infty \frac{[\nu_{\text{SCD}}-\gamma_{\text{SCD}}(v)-i\delta_{\text{SCD}}(v)]f(v)dv}{i\omega+\nu_{\text{SCD}}+\gamma_{\text{D}}(v)+i\delta_{\text{D}}(v)}. \tag{A4}$$

In the limit $|[\gamma_{\text{D}}(v)+i\delta_{\text{D}}(v)]/[i\omega+\nu]|\ll 1$, $S(\omega)$ and $R(\omega)$ can be developed in terms of successive powers of this quantity leading, at the first-order correction, to [10]

$$\mathcal{A}(\omega)=i\omega+\langle\gamma_{\text{D}}\rangle+i\langle\delta_{\text{D}}\rangle+\frac{\Delta^2\delta_{\text{D}}}{i\omega+\nu_{\text{SC}}}+\cdots \tag{A5}$$

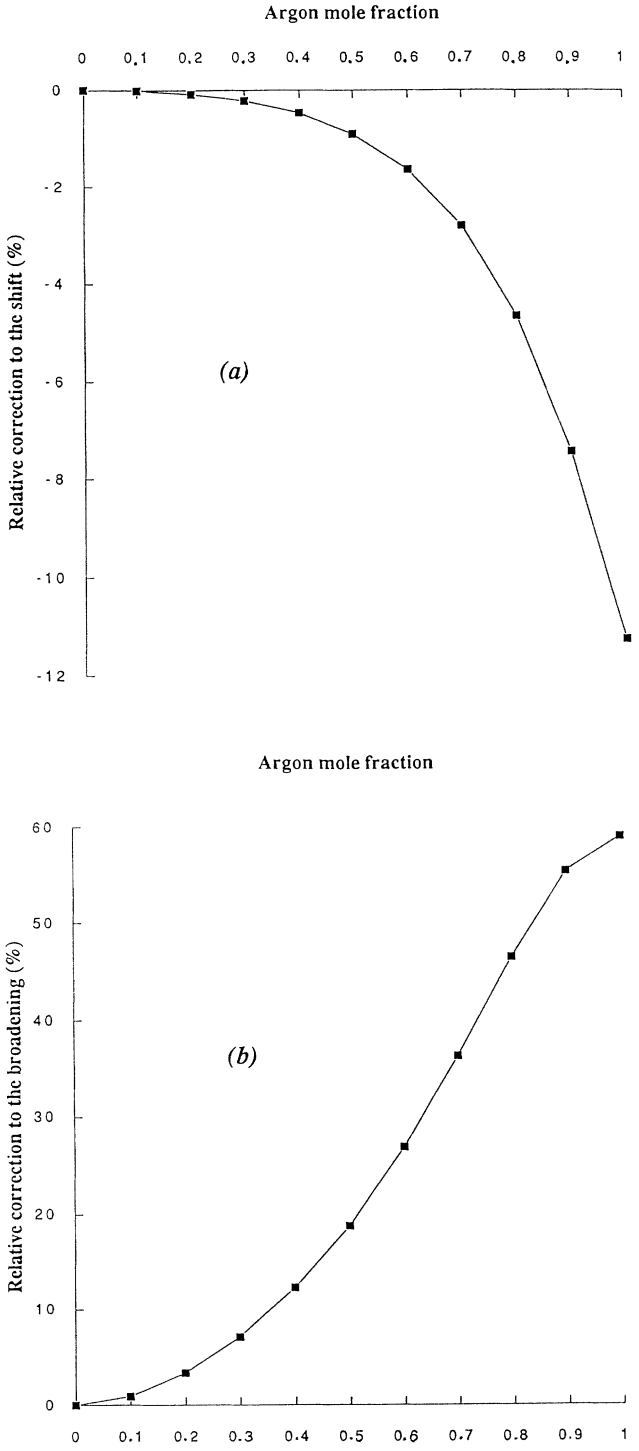

FIG. 9. Relative first-order corrections to (a) the shift and (b) the broadening, introduced by the FRSR model if compared to a Lorentzian profile.

with

$$\Delta^2\delta_D=\langle\delta_D^2\rangle-\langle\delta_D\rangle^2$$

and

$$\mathcal{B}(\omega)=i\omega+\langle\gamma_{coll}\rangle+i\langle\delta_{coll}\rangle+\frac{(1-x)}{x}\frac{\Delta^2\delta_{SCD}}{i\omega+\nu_{SCD}}+\cdots \quad \text{(A6)}$$

with

$$\Delta^2\delta_{SCD}=\langle\delta_{SCD}^2\rangle-\langle\delta_{SCD}\rangle^2 .$$

The resulting profiles are then

$$I_{FRSR}(\omega)=\frac{\langle\gamma_D\rangle+\dfrac{\nu_{SC}\Delta^2\delta_D}{\omega^2+\nu_{SC}^2}}{\left[\omega+\langle\delta_D\rangle-\dfrac{\omega\Delta^2\delta_D}{\omega^2+\nu_{SC}^2}\right]^2+\left[\langle\gamma_D\rangle+\dfrac{\nu_{SC}\Delta^2\delta_D}{\omega^2+\nu_{SC}^2}\right]^2} , \quad \text{(A7)}$$

$$I_{RTBT}(\omega)=\frac{\langle\gamma_{coll}\rangle+\left[\dfrac{1-x}{x}\right]\dfrac{\nu_{SCD}\Delta^2\delta_{SCD}}{\omega^2+\nu_{SCD}^2}}{\left[\omega+\langle\delta_{coll}\rangle-\left[\dfrac{1-x}{x}\right]\dfrac{\omega\Delta^2\delta_{SCD}}{\omega^2+\nu_{SCD}^2}\right]^2+\left[\langle\gamma_{coll}\rangle+\left[\dfrac{1-x}{x}\right]\dfrac{\nu_{SCD}\Delta^2\delta_{SCD}}{\omega^2+\nu_{SCD}^2}\right]^2} . \quad \text{(A8)}$$

As expected, Eq. (A8) describes a Lorentzian profile for $x=1$, i.e., when only SCD collisions are efficient; Eq. (A7) gives asymptotically the same result for high-speed-changing collision frequency.

The relative first-order correction for the shift and the width in the two models considered may be expressed simply in the limit case for which $\langle\delta_D\rangle\gg\langle\gamma_D\rangle$ (or $\langle\delta_{coll}\rangle\gg\langle\gamma_{coll}\rangle$) by taking $\omega\approx-\langle\delta_D\rangle$ (or $\omega\approx-\langle\delta_{coll}\rangle$). This approximation thus consists of considering an equivalent Lorentzian line accounting for the speed effect practically centered on the maximum of the experimental line. It results in

$$\frac{\langle\delta_D^{(1)}\rangle}{\langle\delta_D\rangle}\cong\frac{\Delta^2\delta_D}{\langle\delta_D\rangle^2+\nu_{SC}^2} ,$$
$$\frac{\langle\delta_{coll}^{(1)}\rangle}{\langle\delta_{coll}\rangle}\cong\left[\frac{1-x}{x}\right]\frac{\Delta^2\delta_{SCD}}{\langle\delta_{coll}\rangle^2+\nu_{SCD}^2} , \quad \text{(A9)}$$

$$\frac{\langle\gamma_D^{(1)}\rangle}{\langle\gamma_D\rangle}\cong\frac{\nu_{SC}}{\langle\gamma_D\rangle}\frac{\langle\delta_D^{(1)}\rangle}{\langle\delta_D\rangle} ,$$
$$\frac{\langle\gamma_{coll}^{(1)}\rangle}{\langle\gamma_{coll}\rangle}\cong\frac{\nu_{SCD}}{\langle\gamma_{coll}\rangle}\frac{\langle\delta_{coll}^{(1)}\rangle}{\langle\delta_{coll}\rangle} . \quad \text{(A10)}$$

For the binary mixture H_2-X, the variance $\Delta^2\delta_D$ is given, in terms of the concentration c_X of the perturber

$$\Delta^2\delta_D=c_X^2[\langle\delta_D^2(H_2-X)\rangle-\langle\delta_D(H_2-X)\rangle^2] , \quad \text{(A11)}$$

where the speed dependence of the shift and width for pure H_2 has been neglected. So, these corrections (A9) and (A10) can be written, through Eq. (A11), as

$$\frac{\langle\delta_D^{(1)}\rangle}{\langle\delta_D\rangle}\cong\frac{c_X^2[\langle\delta_D^2(H_2-X)\rangle-\langle\delta_D(H_2-X)\rangle^2]}{(1-c_X)^2\Delta(H_2)+c_X^2\Delta(X)+2c_X(1-c_X)\Delta(H_2-X)} , \quad \text{(A12)}$$

where

$$\Delta(H_2)=[\delta_D^2(H_2-H_2)+\nu_{SC}^2(H_2-H_2)] , \quad \Delta(X)=[\delta_D^2(H_2-X)+\nu_{SC}^2(H_2-X)] ,$$
$$\Delta(H_2-X)=[\delta_D(H_2-H_2)\delta_D(H_2-X)+\nu_{SC}(H_2-H_2)\nu_{SC}(H_2-X)] ,$$

and

$$\frac{\langle\gamma_D^{(1)}\rangle}{\langle\gamma_D\rangle}\cong\left[\frac{(1-c_X)\nu_{SC}(H_2-H_2)+c_X\nu_{SC}(H_2-X)}{(1-c_X)\gamma_D(H_2-H_2)+c_X\gamma_D(H_2-X)}\right]\frac{\langle\delta_D^{(1)}\rangle}{\langle\delta_D\rangle} . \quad \text{(A13)}$$

Similar expressions hold for $\langle \delta_{coll}^{(1)} \rangle / \langle \delta_{coll} \rangle$ and $\langle \gamma_{coll}^{(1)} \rangle / \langle \gamma_{coll} \rangle$.

The numerical estimation of these corrections requires the calculation of the quadratic average shift for the H_2-X pair from Eq. (17). Using the numerical parameters for B and C from Table IV and the γ_D and ν_D values from Table V, the resulting relative corrections at room temperature are shown in Fig. 9 for H_2-Ar as a function of concentration. For this physical situation, the approximation $\langle \delta_D \rangle \gg \langle \gamma_D \rangle$ is realistic. As expected, the shift correction is negative and negligible for concentrations of argon lower than 50% (less than 1% at 295 K). It remains a perturbative correction for higher concentrations (less than 10%). This explains the origin of the correction introduced through the use of the gravity center of the line (first-order moment) to compensate the first-order correction $\langle \delta_D^{(1)} \rangle$. Let us note that the negative sign of the first-order correction $\langle \delta_D^{(1)} \rangle$ implies a super-Lorentzian behavior in the high-frequency wing consistent with the experiments. The approximation $\delta_G \cong \langle \delta_D \rangle$ is thus realistic and leads to a remarkable linearity vs concentration (cf. Fig. 3).

In contrast, the width correction must be accounted for any significant concentration of argon. It is nonperturbative at high concentration (Fig. 9). The origin of this difference is straightforward from Eq. (A13) since the collision frequency term in the numerator of Eq. (A10) is typically one order of magnitude higher than the broadening term in the denominator.

[1] R. H. Dicke, Phys. Rev. **89**, 472 (1953).
[2] L. Galatry, Phys. Rev. **122**, 1218 (1961).
[3] P. R. Berman, Phys. Rev. A **5**, 927 (1972).
[4] P. Lallemand, P. Simova, and G. Brett, Phys. Rev. Lett. **17**, 1239 (1966).
[5] J. R. Murray and A. Javan, J. Mol. Spectrosc. **29**, 502 (1969); **42**, 1 (1972).
[6] A. D. May, V. Degen, J. C. Sryland, and H. L. Welsh, Can. J. Phys. **39**, 1769 (1961); A. D. May, G. Varghese, J. C. Stryland, and H. H. Welsh, Can. J. Phys. **42**, 1058 (1964).
[7] R. L. Farrow, L. A. Rahn, G. O. Sitz, and G. J. Rosasco, Phys. Rev. Lett. **63**, 746 (1989).
[8] D. Robert, J. M. Thuet, J. Bonamy, and S. Temkin, Phys. Rev. A **47**, 771 (1993).
[9] S. G. Rautian and I. I. Sobel'man, Usp. Fiz. Nauk **90**, 209 (1967) [Sov. Phys. Usp. **9**, 701 (1967).
[10] J. M. Thuet, thèse de doctorat, Université de Franche-Comté, Besançon, France, 1993.
[11] J. H. Dymond and E. B. Smith, *The Virial Coefficients of Pure Gases and Mixtures* (Clarendon, Oxford, 1980).
[12] S. Perez, H. Smiedel, and B. Schramm, Z. Phys. Chem. **123**, 35 (1980).
[13] J. O. Hirschfelder, C. F. Curtiss, and R. B. Bird, *Molecular Theory of Gases and Liquids* (Wiley, New York, 1964).
[14] W. K. Bischel and M. J. Dyer, Phys. Rev. A **33**, 3113 (1986).
[15] L. A. Rahn and G. J. Rosasco, Phys. Rev. A **41**, 3698 (1990).
[16] P. Lallemand and P. Simova, J. Mol. Spectrosc. **26**, 262 (1968).
[17] D. Robert, J. Bonamy, J. P. Sala, G. Levi, and F. Marsault-Herail, Chem. Phys. Lett. **99**, 303 (1985).
[18] L. A. Rahn, R. L. Farrow, and G. J. Rosasco, Phys. Rev. A **43**, 6075 (1991).
[19] H. M. Pickett, J. Chem. Phys. **73**, 6090 (1980).
[20] *Handbook of Mathematical Functions*, edited by M. Abramowitz and I. A. Stegun (Dover, New York, 1964).
[21] D. Robert, J. Bonamy, F. Marsault-Herail, G. Levi, and J. P. Marsault, Chem. Phys. Lett. **74**, 467 (1980).
[22] S. Green, J. Chem. Phys. **93**, 1496 (1990).
[23] R. J. Le Roy and J. M. Hutson, J. Chem. Phys. **86**, 837 (1987).
[24] S. Green, J. Chem. Phys. **92**, 4679 (1990).
[25] W. Meyer, P. C. Hariharan, and W. Kutzelnigg, J. Chem. Phys. **73**, 1880 (1980).
[26] S. Green, L. Monchick, and R. Blackmore, J. Chem. Phys. **91**, 52 (1989).
[27] R. Blackmore, S. Green, and L. Monchick, J. Chem. Phys. **91**, 3846 (1989).
[28] S. Green, J. Chem. Phys. **82**, 4548 (1985).